Bouri, Elie; Gabauer, David; Gupta, Rangan et al.

Book

Geopolitical risk and inflation spillovers across European and North American economies

Provided in Cooperation with:
University of Pretoria

Geopolitical Risk and Inflation Spillovers across European and North American Economies

Elie Bouri
Lebanese American University
David Gabauer
Software Competence Center Hagenberg
Rangan Gupta
University of Pretoria
Harald Kinateder
University of Passau

Geopolitical Risk and Inflation Spillovers across European and North American Economies

Elie Bouri[†], David Gabauer[‡], Rangan Gupta[§], and Harald Kinateder[¶,*]

[†]*School of Business, Lebanese American University, Beirut, Lebanon. Email: elie.bouri@lau.edu.lb.*
[‡]*Software Competence Center Hagenberg, Hagenberg, Austria. Email: david.gabauer@scch.at.*
[§]*Department of Economics, University of Pretoria, Pretoria, South Africa. Email: rangan.gupta@up.ac.za.*
[¶,*]*School of Business, Economics and Information Systems, University of Passau, Germany. Email: harald.kinateder@uni-passau.de.*
[*]*Corresponding author.*

Abstract

In this paper, we examine the spillover across the monthly inflation rates (measured by the CPI) covering the USA, Canada, UK, Germany, France, Netherlands, Belgium, Italy, Spain, Portugal, and Greece. Using data covering the period from May 1963 to November 2022 within a time-varying spillover approach, we show that the total spillover index across the inflation rates spiked during the war in Ukraine period, exceeding its previous peak shown during the 1970s energy crisis. Notably, we apply a quantile-on-quantile regression and reveal that the total spillover index is positively associated with the level of global geopolitical risk (GPR) index. Levels of GPR are positively influencing high levels of the inflation spillover index, whereas the GPR Acts index is positively associated with all levels of inflation spillover index. Given that rising levels of inflation are posing risks to the financial system and economic growth, these findings should matter to the central banks and policymakers in advanced economies. They suggest that the policy response should go beyond conventional monetary tools by considering the political actions necessary to solve the Russia-Ukraine war and ease the global geopolitical tensions.

Keywords: Inflation spillovers; geopolitical risk; TVP-VAR; dynamic connectedness.
JEL codes: C32; C5; G15.

1   Introduction

After almost two decades of low and stable inflation, inflationary pressures have started to build up after Q12020 following the COVID-19-induced lockdowns which have led to a shortage of goods and labor in the supply chain. The recent spike in various commodity prices in the wake of the Russia-Ukraine war has aggravated the situation and raised long-term inflation expectations. In fact, the war has disrupted the supply of energy, fertilizers, and grains, and the sanctions on Russia adversely affected trade and production, which further heightens prices. Recent figures show that global inflation has increased from around 2% to more than 6%, reaching high levels not experienced in 40 years well above the inflation targets of monetary authorities in major economies. The situation is often compared to the inflation shock of 1970s, suggesting a possible material risk. As a remedy to high inflation, the Federal Reserve and other central banks in Canada and Europe responded by sharply tightening monetary policy from early 2022, although they have a good history of reacting to economic and political uncertainty by reducing interest rates. Therefore, central banks face a long-term quest of ensuring both price stability and financial system stability, which has been historically very challenging. On the financial markets scene, given that current levels of inflation are high and driven by output shocks that reduce economic capacity, asset returns will not easily absorb inflation and will likely respond negatively.[1]

Under such a challenging environment, it is relevant to participate in the current debate on the supply-led inflation and the role of geopolitical risk. Notably, a major concern of monetary policy is to understand the spillover effect of inflation across major economies, which might have implications on domestic consumer prices and monetary policy design. For example, if linkages among global inflation rates are the result of common (geopolitical) shocks, then central banks have to jointly (and not) independently fight inflation (Jordan, 2016). However, recent studies on the linkage of inflation rates across economies are limited in their sample period, scope, and the factors driving it. Pham and Sala (2022) focus G7 plus Spain using monthly data from 1991 to 2019 and

---

[1]This is the opposite of the case of low levels of inflation and expected inflation, which is not necessarily harmful to asset prices. However, there have been a few exceptions where stock prices and inflation were positively correlated, see Antonakakis et al. (2017).

the Diebold/Yılmaz approach. They provide evidence that the level of connectedness in inflation is stronger than the level of connectedness in unemployment although both vary across time and increase during crisis periods such as the 2008 Global Financial Crisis. Using Euro-area monthly data from January 1955 to April 2017, Tiwari et al. (2019) apply time and frequency measures of spillovers and show that Germany is a major inflation transmitter unlike Spain which acts as an inflation receiver. Furthermore, they indicate that the inflation rates are significantly correlated in the long-term and increase with the time-scales. In a recent study, Aharon and Qadan (2022) consider G7 economies with a time-varying spillover approach. They report an increase in the connectedness across the inflation rates of G7 countries during the pandemic and Russia-Ukraine war. However, their data sample period is not comprehensive, notably because (i) its sample period is limited to January 1990-May 2022 and (ii) the sample covers only U.K., France, Germany, Italy, only, despite the fact that the war shock particularly concerns most of European countries. In this regard, European countries are harshly influenced by trade disruptions, especially because they rely on energy imports from Russia, which include natural gas, (35%), crude oil, (20%), and coal (40%).[2] Furthermore, the scope of the analysis of Aharon and Qadan (2022) is limited to the spillover effect across inflation rates and does not pay attention to the role of geopolitical risk as a potential driver of inflation spillovers. Such issues are very important, as highlighted by the recent study of Caldara et al. (2023), which uses a structural VAR model on monthly data from the 1970s and shows that global geopolitical risks upsurge the level of inflation in many countries.

Based on the above, the academic literature remains unclear how inflation is spilled over across North American and European economies over time covering the periods of great inflation of 1970s, the COVID-19 outbreak, and the Russia-Ukraine war. Furthermore, it is silent about the role GPR in driving the spillover effect across the inflation rates of these economies and whether this role is more or less strong under high levels of geopolitical risk.

In this paper, we examine the spillover effect across the monthly inflation rates of the USA, Canada, UK, Germany, France, Netherlands, Belgium, Italy, Spain, Portugal, and Greece and relates it to global geopolitical risk. To this end, we first use a time-varying

---

[2]https://blogs.worldbank.org/developmenttalk/commodity-prices-surge-due-war-ukraine.

spillover framework on monthly inflation rates data for the period May 1963 to November 2022, and then conduct a quantile-on-quantile regression to understand the impact of various (low, moderate, and high) levels of geopolitical risk on the various states (low, moderate, and high) of inflation spillovers.

The results show that the total spillover index across the inflation rates spiked during the war in Ukraine period, exceeding its previous peak shown during the 1970s energy crisis. Notably, we apply a quantile-on-quantile regression and reveal that the total spillover index is positively associated with the level of global geopolitical risk, whereas only high levels of GPR Acts index are positively associated with all levels of inflation spillover index. Our paper contributes to the related literature on three fronts. Firstly, it examines the spillover effect across inflation rates from a large sample comprising various economies from North America and Europe, unlike most previous studies that are generally centered on the US or G7 economies (Saâdaoui et al. (2022); Caldara et al. (2023); Shahzad et al. (2023)). Secondly, it provides insights on the level of inflation transmission over a long sample period from before 1970s, covering output shocks such as the COVID-19 and Russia-Ukraine war, which enriches the current literature (for example, Pham and Sala (2022)). In line with previous results, we show that the spillover of inflation intensifies during crisis periods (Aharon and Qadan, 2022). Thirdly, it considers the role of geopolitical risk in driving inflation spillovers, showing that heightened geopolitical risk can drive higher the inflation spillover effect. Geopolitical risk is a contributor to inflation spillovers among advanced economies, suggesting that inflation is not a domestic problem but rather a global phenomenon shared by major economies; importantly, the dynamic of inflation spillovers is driven by geopolitical risk. Previous studies indicate that geopolitical stability has been the backbone of the decades-long efficient resource allocation and disinflation. Accordingly, our results point to a synchronization of inflation rates across North American and European economies under the geopolitical led inflation, which provides useful insights on the behavior of inflation and the policies suitable to curb inflation.

The remainder of this study is structured as follows: Section 2 describes the underlying data. Section 3 outlines the employed methodology. Section 4 presents the empirical results while Section 5 discusses their implications. Finally, Section 6 concludes the study.

2 Data

In this study, we examine the monthly inflation transmission mechanism between the United States of America (USA), Canada (CAN), Great Britain (GBR), Germany (DEU), Belgium (BEL), the Netherlands (NLD), France (FRA), Italy (ITA), Spain (ESP), Portugal (PRT), and Greece (GRC) over the period from May 1963 to November 2022. In more detail, we use non-seasonally adjusted consumer price indices that are obtained from the *Federal Reserve Economic Database*[3] and compute the year-over-year (YoY) inflation rates by $z_{it} = \frac{x_{it} - x_{it-12}}{x_{it-12}}$, where z_{it} is the year-over-year inflation rate and x_{it} and is the non-seasonally adjusted consumer price index of country i. The YoY inflation rates are illustrated in Figure 1.

[INSERT FIGURE 1 AROUND HERE.]

Table 1 shows the summary statistics of the inflation rates. We see the largest average inflation rates occurred in PRT, followed by GRC, ESP, ITA, and IRE while the lowest average inflation rates are associated with DEU, NLD, BEL, CAN, and USA. Also, when it comes to the variability of inflation rates, we see that GRC, ITA, PRT and ESP are again on the upper end while DEU, BEL, NLD, USA, and CAN are on the lower end. Notably, we find that all inflation rates are significantly right-skewed and leptokurtic distributed. Thus, we also find that all series are not normally distributed according to the Jarque and Bera (1980) normality test. Additionally, the summary statistics also point out that all inflation rates are autocorrelated and exhibit ARCH/GARCH errors (Fisher and Gallagher, 2012) at least at the 1% significance level as well as stationary at least at the 7% significance level. Finally, we also see that all Kendall correlation coefficients are significantly positive with the lowest correlation occurring between NLD and GRC (0.230) while the largest correlation is present between ITA and ESP (0.760). Thus, modeling the interdependencies using a TVP-VAR with a time-varying variance-covariance structure appears to be an adequate choice.

[INSERT TABLE 1 AROUND HERE.]

---

[3]The exact tickers are "{CC}CPIALLMINMEI" where $\{CC\}$ stands for the three-letter country codes defined in ISO 3166-1.

As far as the metric of GPR is concerned, we rely on the index developed by Caldara and Iacoviello (2022).[4] The GPR (historical) index reflects automated text-search results of the electronic archives of 3 newspapers namely, the Chicago Tribune, the New York Times, and the Washington Post. Caldara and Iacoviello (2022) calculate the index by counting the number of articles related to adverse geopolitical events in each newspaper for each month (as a share of the total number of news articles). The search is organized in eight categories: War Threats, Peace Threats, Military Buildups, Nuclear Threats, Terror Threats, Beginning of War, Escalation of War, and Terror Acts. We further consider a subvariant of the GPR index, namely the GPR Acts index, which only reflects phrases related to the realization or escalation of adverse events such as starting or escalation of a war and terrorist acts.

3 Methodology

3.1 TVP-VAR-based connectedness approach

In order to examine the inflation transmission mechanism, we employ the time-varying parameter (TVP) vector autoregressive (VAR) model based extended joint connectedness approach introduced by Balcilar et al. (2021). This framework combines the advantages of the following proposed connectedness frameworks: Diebold and Yılmaz (2012, 2014), Antonakakis et al. (2020), and Lastrapes and Wiesen (2021). In Diebold and Yılmaz (2012, 2014) the original static and dynamic (rolling-window) VAR-based connectedness framework has been introduced. Antonakakis et al. (2020) refined this framework by introducing TVP-VAR-based connectedness measures which (i) track changes in the parameters faster and more accurately, (ii) are less outlier sensitive, (iii) do not lose observations, and (iv) can be employed when dealing with low-frequency datasets. Part of these advantages is caused by the structure of the TVP-VAR model while other advantages such as the more accurate capturing of parameter changes have been verified by using different Monte Carlo simulations. Finally, Lastrapes and Wiesen (2021) has introduced the concept of joint connectedness measures which use a more sophisticated and adequate GFEVD normalization technique as the originally proposed row normalization technique

---

[4]The data is available for download from: https://www.matteoiacoviello.com/gpr.htm.

(see, Diebold and Yilmaz, 2012). However, the initial proposition had the disadvantage that it could not compute net pairwise directional connectedness measures. In the work of Balcilar et al. (2021), the joint connectedness approach has been extended in order to compute the net pairwise directional connectedness measures and pairwise connectedness indices (Gabauer, 2021; Chatziantoniou and Gabauer, 2021) in the fashion of the TVP-VAR framework. As the TVP-VAR-based extended joint connectedness approach depends on the TVP-VAR-based connectedness approach (Antonakakis et al., 2020), we have to first describe the original approach and later on how the total connectedness index (TCI) of the TVP-VAR-based connectedness approach is used to weight the connectedness measure in the extended joint connectedness framework.

We start with outlining the TVP-VAR(1) model as suggested by the Bayesian information criterion (BIC):

$$\boldsymbol{z}_t = \boldsymbol{B}_t \boldsymbol{z}_{t-1} + \boldsymbol{u}_t \qquad\qquad \boldsymbol{u}_t \sim N(\boldsymbol{0}, \boldsymbol{S_t}) \tag{1}$$

$$vec(\boldsymbol{B}_t) = vec(\boldsymbol{B}_{t-1}) + \boldsymbol{v}_t \qquad\qquad \boldsymbol{v}_t \sim N(\boldsymbol{0}, \boldsymbol{R}_t) \tag{2}$$

where $\boldsymbol{z}_t$, $\boldsymbol{z}_{t-1}$ and $\boldsymbol{u}_t$ are $k \times 1$ dimensional vectors in t, $t-1$, and the corresponding error term, respectively. $\boldsymbol{B}_t$ and $\boldsymbol{S}_t$ are $k \times k$ dimensional matrices demonstrating the TVP-VAR coefficients and the time-varying variance-covariance while $vec(\boldsymbol{B}_t)$ and $\boldsymbol{v}_t$ are $k^2 \times 1$ dimensional vectors and $\boldsymbol{R}_t$ is a $k^2 \times k^2$ dimensional matrix.

In the next step, the TVP-VAR is transformed to its TVP-VMA representation using the Wold representation theorem: $\boldsymbol{z}_t = \sum_{i=1}^{p} \boldsymbol{B}_{it} \boldsymbol{z}_{t-i} + \boldsymbol{u}_t = \sum_{j=0}^{\infty} \boldsymbol{A}_{jt} \boldsymbol{u}_{t-j}$.

Subsequently, the TVP-VMA coefficients are used to compute the generalized forecast error variance decomposition (GFEVD) of Koop et al. (1996) and Pesaran and Shin (1998). The H-step ahead GFEVD models the impact a shock in series j has on series i. This can be formulated as follows,

$$\phi_{ij,t}^{gen}(H) = \frac{\sum_{h=0}^{H-1}(\boldsymbol{e}_i' \boldsymbol{A}_{ht} \boldsymbol{S}_t \boldsymbol{e}_j)^2}{(\boldsymbol{e}_j' \boldsymbol{S}_t \boldsymbol{e}_j)\sum_{h=0}^{H-1}(\boldsymbol{e}_i' \boldsymbol{A}_{ht} \boldsymbol{S}_t \boldsymbol{A}_{ht}' \boldsymbol{e}_i)} \tag{3}$$

$$gSOT_{ij,t} = \frac{\phi_{ij,t}^{gen}(H)}{\sum_{l=1}^{k} \phi_{ik,l}^{gen}(H)} \tag{4}$$

where $\boldsymbol{e}_i$ is a $k \times 1$ dimensional zero vector with unity on its ith position. As $\phi_{ij,t}^{gen}(H)$

stands for the unscaled GFEVD ($\sum_{j=1}^{k} \phi_{ij,t}^{gen}(H) \neq 1$), Diebold and Yılmaz (2009, 2012, 2014) normalize $\phi_{ij,t}^{gen}(H)$ by dividing it by each row sum to obtain the scaled GFEVD, $gSOT_{ij,t}$.

The scaled GFEVD is at the center of the connectedness approach allowing the computation of the total directional connectedness TO (FROM) all other series. While the TO total directional connectedness demonstrates the impact series i has on all others, the FROM total directional connectedness illustrates the effect all series have on series i. Those measures are computed as follows,

$$S_{i\to\bullet,t}^{gen,to} = \sum_{j=1,i\neq j}^{k} gSOT_{ji,t} \tag{5}$$

$$S_{i\leftarrow\bullet,t}^{gen,from} = \sum_{j=1,i\neq j}^{k} gSOT_{ij,t}. \tag{6}$$

By computing the difference between the TO and the FROM total directional connectedness we obtain the net total directional connectedness. This indicator reports whether series i is a net transmitter or receiver of shocks. If $S_{i,t}^{gen,net} > 0$ ($S_{i,t}^{gen,net} < 0$), series i is influencing (influenced by) all others more than being influenced by (influencing) them, series i is considered a net transmitter (receiver) of shocks indicating that series i is driving (driven by) the network:

$$S_{i,t}^{gen,net} = S_{i\to\bullet,t}^{gen,to} - S_{i\leftarrow\bullet,t}^{gen,from} \tag{7}$$

Another relevant metric in the connectedness literature is the TCI which highlights the degree of network interconnectedness and hence market risk. Mathematically, the TCI is the average total directional connectedness to (from) others and thus equal to the average amount of spillovers one series transmits (receives) from all others:

$$gSOI_t = \frac{1}{K}\sum_{i=1}^{k} S_{i\leftarrow\bullet,t}^{gen,from} = \frac{1}{K}\sum_{i=1}^{k} S_{i\to\bullet,t}^{gen,to}, \tag{8}$$

It should be noted that a high (low) TCI indicates high (low) market risk.

Finally, we focus on the net pairwise directional connectedness which demonstrates

the bilateral transmission between series i and j,

$$S_{ij,t}^{gen,net} = gSOT_{ji,t}^{gen,to} - gSOT_{ij,t}^{gen,from}. \tag{9}$$

If $S_{ij,t}^{gen,net} > 0$ ($S_{ij,t}^{gen,net} < 0$), series i dominates (is dominated) series j indicating that series i influences (is influenced by) series j more than being influenced by (influencing) it.

3.2 Extended joint connectedness approach

When turning to the extended joint connectedness approach, the main advantage over the connectedness approach of Diebold and Yılmaz (2012, 2014) is that the normalization method has been derived from econometric theory[5]. $S_{i\leftarrow\bullet,t}^{jnt,from}$ illustrates the impact all series have on series i. This can be formulated as follows,

$$\boldsymbol{\xi}_t(H) = \boldsymbol{z}_{t+H} - E(\boldsymbol{z}_{t+H}|\boldsymbol{z}_t, \boldsymbol{z}_{t-1}, ...) = \sum_{h=0}^{H-1} \boldsymbol{A}_{h,t}\boldsymbol{\epsilon}_{t+H-h} \tag{10}$$

$$E(\boldsymbol{\xi}_t(H)\boldsymbol{\xi}_t'(H)) = \boldsymbol{A}_{h,t}\boldsymbol{S}_t\boldsymbol{A}_{h,t}' \tag{11}$$

$$S_{i\leftarrow\bullet,t}^{jnt,from} = \frac{E(\xi_{i,t}^2(H)) - E[\xi_{i,t}(H) - E(\xi_{i,t}(H))|\epsilon_{\forall\neq i,t+1}, ..., \epsilon_{\forall\neq i,t+H}]^2}{E(\xi_{it}^2(H))} \tag{12}$$

$$= \frac{\sum_{h=0}^{H-1} \boldsymbol{e}_i'\boldsymbol{A}_{ht}\boldsymbol{\Sigma}_t\boldsymbol{M}_i(\boldsymbol{M}_i'\boldsymbol{\Sigma}_t\boldsymbol{M}_i')^{-1}\boldsymbol{M}_i'\boldsymbol{\Sigma}_t\boldsymbol{A}_{ht}'\boldsymbol{e}_i}{\sum_{h=0}^{H-1} \boldsymbol{e}_i'\boldsymbol{A}_{ht}\boldsymbol{\Sigma}_t\boldsymbol{A}_{ht}'\boldsymbol{e}_i} \tag{13}$$

where $\boldsymbol{M}_i$ is a $K \times K - 1$ rectangular matrix that equals the identity matrix with the ith column eliminated, and $\boldsymbol{\epsilon}\forall \neq i, t+1$ denotes the $K - 1$-dimensional vector of shocks at time $t+1$ for all series except series i.

In the next step, the joint total connectedness index is computed by,

$$jSOI_t = \frac{1}{K} \sum_{i=1}^{k} S_{i\leftarrow\bullet,t}^{jnt,from}. \tag{14}$$

This metric is within zero and unity as opposed to the TCI of the originally proposed approach (see, Chatziantoniou and Gabauer, 2021; Gabauer, 2021).

An important extension of Balcilar et al. (2021) is that multiple scaling factors are

---

[5]For detailed mathematical derivations interested readers are referred to the technical appendix of Lastrapes and Wiesen (2021).

used to relate $gSOT$ to $jSOT$:

$$\lambda_{it} = \frac{S_{i\leftarrow\bullet,t}^{jnt,from}}{S_{i\leftarrow\bullet,t}^{gen,from}} \tag{15}$$

$$jSOT_{ij,t} = \lambda_{it} gSOT_{ij,t} \tag{16}$$

Based upon this equality, the total directional connectedness from series i to all others, the net total directional, and the net pairwise directional connectedness measures can be calculated as follows,

$$S_{i\rightarrow\bullet,t}^{jnt,to} = \sum_{j=1,i\neq j}^{k} jSOT_{ji,t} \tag{17}$$

$$S_{j,t}^{jnt,net} = S_{i\rightarrow\bullet,t}^{jnt,to} - S_{\bullet\rightarrow i,t}^{jnt,from} \tag{18}$$

$$S_{ij,t}^{jnt,net} = jSOT_{ji,t}^{jnt,to} - jSOT_{ij,t}^{jnt,from}. \tag{19}$$

3.3 Quantile-on-quantile approach

After having obtained the time-varying total connectedness series from the TVP-VAR model, we use the quantile-on-quantile (QQ) approach of Sim and Zhou (2015) to examine the relationship between the inflation interconnectedness and the geopolitical risk index of Caldara and Iacoviello (2022). The QQ model can be outlined as follows,

$$\Delta TCI_t = \beta^\theta(\Delta GPR_{t-1}) + u_t^\theta \tag{20}$$

where ΔTCI_t and ΔGPR_{t-1} are the quarter-on-quarter changes of the total connectedness index and the geopolitical risk in period $t-1$, respectively. θ stands for the θ-th quantile of the conditional distribution of the ΔTCI and u_t^θ is a quantile error term whose conditional θ-th quantile is equal to zero. The term $\beta^\theta(\cdot)$ is assumed to be of unknown functional form, which is to be determined via the employed dataset.

Using a standard quantile regression model (see, Equation (20)) allows to measure the impact ΔGPR_{t-1} to vary across the different quantiles on the inflation interconnectedness, however, this model is unable to capture the dependence in its entirety as the term $\beta^\theta(\cdot)$ is indexed on the TCI quantiles (θ) only and not the quantiles of the ΔGPR_{t-1}. Therefore, in order to get more comprehensive insights into the effect of ΔGPR_{t-1} on the connectedness

of inflation, we focus on the relationship between the θ-th quantile of the TCI and the τ-th quantile of the ΔGPR_{t-1}, denoted by P^τ. This is done by examining Equation (20) in the neighborhood of P^τ via a local linear regression. As $\beta^\theta(\cdot)$ is unknown, this function is approximated through a first-order Taylor expansion around a quantile P^τ, such that

$$\beta^\theta(P_t) \approx \beta^\theta(P^\tau) + \beta^{\theta'}(P^\tau)(P_t - P^\tau) \tag{21}$$

where $\beta^{\theta'}$ is the partial derivative of $\beta^\theta(P_t)$ with respect to P and is similar in its interpretation to the coefficient (slope) of a linear regression model. Next, renaming $\beta^\theta(P^\tau)$ and $\beta^{\theta'}(P^\tau)$ as $\beta_0(\theta, \tau)$ and $\beta_1(\theta, \tau)$ respectively, we rewrite equation (21) as

$$\beta^\theta(P_t) \approx \beta_0(\theta, \tau) + \beta_1(\theta, \tau)(P_t - P^\tau) \tag{22}$$

By substituting Equation (22) into Equation (20), we obtain

$$T_t = \underbrace{\beta_0(\theta, \tau) + \beta_1(\theta, \tau)(P_t - P^\tau)}_{(*)} + u_t^\theta \tag{23}$$

where the term $(*)$ is the θ-th conditional quantile of the TCI. Unlike the standard conditional quantile function, Equation (23) captures the overall dependence structure between the θ-th quantile of the ΔTCI_t and the τ-th quantile of the ΔGPR_{t-1} as the parameters β_0 and β_1. In the estimation of Equation (23), $\hat{P}_t$ and $\hat{P}^\tau$, as well as, the local linear regression estimates of the parameters $\hat{\beta}_0$ and $\hat{\beta}_1$ are obtained by solving the following minimization problem,

$$\min_{b_0, b_1} = \sum_{i=1}^n \rho_\theta \left[T_t - \hat{\beta} - \hat{\beta}_1(\hat{P}_t - \hat{P}^\tau) \right] K \left(\frac{F_n(\hat{P}_t - \tau)}{h} \right) \tag{24}$$

where $\rho(u)$ is the quantile loss function, defined as $\rho(u) = u(\theta - I(u < 0))$ and I is an indicator function. $K(\cdot)$ demonstrates a kernel function while h is the bandwidth parameter of the kernel. Caused by its computational simplicity and efficiency, the Gaussian kernel is employed to weight the observations in the neighborhood of P^τ. It should be noted that these weights are inversely related to the distance between the empirical distribution function of $\hat{P}_t$, denoted by $F_n(\hat{P}_t) = \frac{1}{n} \sum_{k=1}^n I(\hat{P}_k < \hat{P}_t)$, and the value of the distribution function which corresponds with the quantile P^τ, denoted by τ. Finally, the value of the

bandwidth parameter h is chosen based on cross-validating the local linear regression.

4 Empirical results

4.1 Averaged connectedness measures

We begin this section by interpreting the averaged connectedness measures which are outlined in Table 2. Diagonal values represent own-variance shares while off-diagonal represent the impact variable j (column) has on variable i (row).

Table 2 highlights the interconnectedness among inflation rates. The averaged TCI stress that on average 70.87% of a shock in one variable is transmitted to all others indicating that inflation rates are highly interconnected and that a shock in one country heavily affects other countries. The main drivers of those spillover shocks are USA (120.51%), FRA (36.05%), DEU (27.81%), and PRT (13.46%) while the main receivers of shocks are NLD (-43.50%), ITA (-43.24%), CAN (-33.20%), GBR (-32.02%), BEL (-25.44%), GRC (-12.29%), and ESP (-8.15%). Having a closer look at the pairwise dynamics reveals that countries which are geographically closer to each other or with substantial trading ties are more interconnected. For instance, CAN highest influence is on the USA. Additionally, the influence of DEU and FRA on neighboring countries is higher than the impact of the USA or CAN.

Interestingly, it appears that we either deal with stronger net shock transmitting or receiving countries as the net pairwise transmission (NPT) which illustrates how many countries country i dominates is either large or small. For instance, we find that USA dominates 9 countries and DEU and PRT dominate 8 other countries. FRA and ESP dominate 5 other countries. On the other hand, NLD and ITA are only driving two other countries.

[INSERT TABLE 2 AROUND HERE.]

Figure 2 illustrates the averaged net pairwise directional connectedness while the magnitude of the net pairwise transmission mechanism is reported in parentheses in Table 2. It is shown that the inflation of ITA is driven by all other countries, expect ESP, as all edges point at ITA and thus ITA is considered as a net receiver of shocks (yellow). The

same is true for BEL which is driven by all other countries except GBR and NLD. On the contrary, USA drives all other countries' inflation rates except for the PRT inflation rate which drives the US one - however, the magnitude of this propagation is small as highlighted by the thin edge. DEU and FRA are further main transmitters of shocks which are only driven by a few countries. Notably, GRC and PRT drive the inflation in several European countries. These findings can be explained by the fact that DEU, FRA, and the USA are among the world's largest economies while GRC and ESP have been the main driver of inflation and risk as the European government debt crisis has shown.

[INSERT FIGURE 2 AROUND HERE.]

4.2 Dynamic connectedness measures

Figure 3 unveils the dynamics of the TCI. We see that the dynamic total connectedness increased during the 1970s illustrating the first and second oil price shocks (1973, 1979), and decreased starting in 1980 during the oil glut period. The peaks in 2008 and 2010 can be associated with the Global Financial Crisis and European government debt crisis, respectively. Finally, we see at the beginning of 2022 a substantial increase in the dynamic total connectedness which is related to the Russia-Ukraine war.

[INSERT FIGURE 3 AROUND HERE.]

4.3 Quantile-on-quantile results

In Figure 4 the quantile-on-quantile relation between TCI and GPR index is illustrated. The QQ relationship points out that high levels of the total spillover index are positively associated with the level of geopolitical risk, especially when the latter is at moderate and high levels, which is in line with the current global scenario, which witnessed high inflation due to the high demand following quantitative easing measures during the COVID-19 outbreak, and this higher initial inflation state was propelled further because of higher GPR emanating from the Russia-Ukraine war and higher oil prices. We further consider the GPR Acts index, which only reflects phrases related to the realization or escalation of adverse events such as starting or escalation of a war and terrorist acts, and the results

presented in Figure 5 show that high levels of the GPR Acts index are positively associated with all levels of the inflation spillover index. This results indicates the particularity of the Acts dimension of global geopolitical risk in driving inflation spillovers, irrespective of the size of the TCI.

[INSERT FIGURE 4 AROUND HERE.]

[INSERT FIGURE 5 AROUND HERE.]

5 Implications

Our results demonstrate that the levels of GPR positively influence inflation spillovers in the Western world. As these countries are not only economically connected but also politically allied, times of geopolitical tensions often imply that there is less free trading and, therefore, increased problems in consumer supply. The current Russia-Ukraine war is an excellent example. Due to sanctions, certain supply chains are disrupted and some products that have been manufactured in Russia and/or its allied countries are no longer available or are available at higher costs. The same applies for raw materials. Another important aspect is that geopolitical tensions can lead to a decline of economic globalization as certain countries are no longer willing to source out key industries such as the semi-conductor or defence branch. Recent findings of Boubaker et al. (2022) show that countries with higher degrees of economic globalization are more vulnerable to geopolitical conflicts. To sum up, in times of high GPR, one would expect higher inflation rates in all Western countries due to lower degree of economic globalization and supply shortages, as well as high inflation spillovers across European and North American countries.

Another important question in this context is what the economic consequences of higher inflation are. As this is not the core topic of this paper, there will be a brief discussion only. Basically, economy theory would expect a negative effect of higher inflation on most companies' stocks as higher inflation rates induce higher interest rates. Given the logic of the discounted cash flow model, higher interest rates increase discounting of future cash flows, resulting in a lower present value or stock price, respectively. However, this rule of thumb does not hold for all sectors. For example, the energy sector

usually booms in times of GPR. Since the beginning of the Russia-Ukraine war, Western oil companies have performed quite well as sanctions do not allow Western countries to buy Russian energy commodities to the same conditions and extent as before the war. Another notable example is the financial sector. On the one hand, rising interest rates are good news for banks, especially in Europe, as they have suffered a lot from the low interest environment in the last decade. Due to higher interest rates, they can earn more on customers' deposits by increasing their margin which is total interest received (i.e. by customers paying interest on loans) minus total interest paid (i.e. by banks paying interest on deposits). The first part of this difference is growing faster than the second as banks are only willing to increase interest payments on customer deposits in a slow manner. One the other hand, rising interest rates can also have a negative impact on banks. In a low interest environment, the hurdle rate for profitable businesses is low. Rising interest rates increase this hurdle rate which makes less business profitable and leads to a higher number of loan defaults. The first banks that will face these problems are those that have financed a larger number of start-ups and other speculative or unprofitable companies. This is exactly the scenario that happened in the US in March 2023. The rapidly rising interest rates have caused two US banks (Silvergate Capital Bank and Silicon Valley Bank) with significant exposure to the technology sector or cryptocurrencies and another one (Signature Bank) to fail.

6 Concluding remarks

In this study, we analyse connectedness between inflation rates of advanced economies in America and Europe using the recently developed TVP-VAR based extended joint connectedness approach of Balcilar et al. (2021). This approach has several advantages compared to previous connectedness approaches as it tracks changes in the parameters faster and more accurately, is less sensitive for outlies, does not lose observations and can be employed for low-frequency data. We find that the level of connectedness between inflation rates is higher during times of GPR. It reached a new peak in 2022 due to the Russian-Ukraine war and increased money supply and government spending during the COVID-19 pandemic. Just before the beginning of the war in years 2020-2021, central

banks' quantitative easing reached unprecedented levels in most Western countries. The quantitative easing measures with the largest extend have been carried out in the US, where the Fed's total assets almost doubled in the COVID-19 period and the government distributed helicopter money to the citizens. This may explains why our results show that the US is the largest transmitter of inflation shocks to other Western countries.

Future research can use these outcomes to provide additional insights in inflation dynamics. Given the connectedness of inflation during times of GPR, one could analyse the existence of certain inflation regimes. The latter can be useful for inflation forecasting and thus help central banks to make adequate monetary policy decisions (Ftiti et al., 2015), since interest rate decisions depend, among other things, on the forecasted inflation rate.

A   Appendix

A.1   Technical Appendix

The TVP-VAR is represented as follows,

$$\boldsymbol{z}_t = \boldsymbol{B}_t \boldsymbol{z}_{t-1} + \boldsymbol{u}_t \qquad\qquad \boldsymbol{u}_t \sim N(\boldsymbol{0}, \boldsymbol{S}_t)$$

$$vec(\boldsymbol{B}_t) = vec(\boldsymbol{B}_{t-1}) + \boldsymbol{v}_t \qquad\qquad \boldsymbol{v}_t \sim N(\boldsymbol{0}, \boldsymbol{R}_t)$$

where $\boldsymbol{z}_t$, $\boldsymbol{z}_{t-1}$, and $\boldsymbol{u}_t$ represent $k \times 1$ dimensional vectors and $\boldsymbol{B}_t$ and $\boldsymbol{S}_t$ are $k \times k$ dimensional matrices. Furthermore, $vec(\boldsymbol{B}_t)$ and $\boldsymbol{v}_t$ are $k^2 \times 1$ dimensional vectors and $\boldsymbol{R}_t$ is an $k^2 \times k^2$ dimensional matrix.

An empirical Bayes prior is applied where the priors, $vec(\boldsymbol{B}_0)$ and $\boldsymbol{S}_0$, are equal to the estimation results of a constant parameter VAR estimation based on the full dataset.

$$vec(\boldsymbol{B}_0) \sim N(vec(\boldsymbol{B}_{OLS}), \boldsymbol{R_{OLS}})$$

$$\boldsymbol{S}_0 = \boldsymbol{S}_{OLS}.$$

The Kalman Filter estimation relies on forgetting factors ($0 \le \kappa_i \le 1$) which regulates how fast the estimated coefficients vary over time. If the forgetting factor is set equal to 1 the algorithm collapses to a constant parameter VAR. Since it is assumed that parameters are not changing dramatically from one day to another, κ_2 is set equal to 0.99:

$$vec(\boldsymbol{B}_t)|\boldsymbol{z}_{1:t-1} \sim N(vec(\boldsymbol{B}_{t|t-1}), \boldsymbol{R}_{t|t-1})$$

$$vec(\boldsymbol{B}_{t|t-1}) = vec(\boldsymbol{B}_{t-1|t-1})$$

$$\boldsymbol{R}_t = (1 - \kappa_2^{-1})\boldsymbol{R}_{t-1|t-1}$$

$$\boldsymbol{R}_{t|t-1} = \boldsymbol{R}_{t-1|t-1} + \boldsymbol{R}_t$$

The multivariate EWMA procedure for $\boldsymbol{S}_t$ is updated in every step, while κ_1 and κ_2 are set equal to 0.99 based on the sensitivity results provided by Koop and Korobilis (2014). Furthermore, Koop and Korobilis (2014) fix the forgetting factors, as well, even if the forgetting factors can be estimated by the data, as in Koop and Korobilis (2013). The main reason to fix the parameters is twofold (i) it increases computational burden

substantially and (ii) the value added to the forecasting performance is questionable.

$$\hat{\boldsymbol{u}}_t = \boldsymbol{z}_t - \boldsymbol{B}_{t|t-1}\boldsymbol{z}_{t-1}$$

$$\boldsymbol{S}_t = \kappa_1 \boldsymbol{S}_{t-1|t-1} + (1-\kappa_1)\hat{\boldsymbol{u}}_t'\hat{\boldsymbol{u}}_t$$

$vec(\boldsymbol{B}_t)$ and $\boldsymbol{R}_t$ are updated by

$$vec(\boldsymbol{B}_t)|\boldsymbol{z}_{1:t} \sim N(vec(\boldsymbol{B}_{t|t}), \boldsymbol{R}_{t|t})$$

$$vec(\boldsymbol{B}_{t|t}) = vec(\boldsymbol{B}_{t|t-1}) + \boldsymbol{R}_{t|t-1}\boldsymbol{z}_{t-1}'(\boldsymbol{S}_t + \boldsymbol{z}_{t-1}\boldsymbol{R}_{t|t-1}\boldsymbol{z}_{t-1}')^{-1}(\boldsymbol{z}_t - \boldsymbol{B}_{t|t-1}\boldsymbol{z}_{t-1})$$

$$\boldsymbol{R}_{t|t} = \boldsymbol{R}_{t|t-1} + \boldsymbol{R}_{t|t-1}\boldsymbol{z}_{t-1}'(\boldsymbol{S}_t + \boldsymbol{z}_{t-1}\boldsymbol{R}_{t|t-1}\boldsymbol{z}_{t-1}')^{-1}(\boldsymbol{z}_{t-1}\boldsymbol{R}_{t|t-1})$$

Finally, the variances, $\boldsymbol{S}_t$, are updated by the EWMA procedure

$$\hat{\boldsymbol{u}}_{t|t} = \boldsymbol{z}_t - \boldsymbol{B}_{t|t}\boldsymbol{z}_{t-1}$$

$$\boldsymbol{S}_{t|t} = \kappa_1 \boldsymbol{S}_{t-1|t-1} + (1-\kappa_1)\hat{\boldsymbol{u}}_{t|t}'\hat{\boldsymbol{u}}_{t|t}$$

References

Aharon, D. Y. and Qadan, M. (2022). Infection, invasion, and inflation: Recent lessons. *Finance Research Letters*, 50:103307.

Anscombe, F. J. and Glynn, W. J. (1983). Distribution Of The Kurtosis Statistic B2 For Normal Samples. *Biometrika*, 70(1):227–234.

Antonakakis, N., Chatziantoniou, I., and Gabauer, D. (2020). Refined measures of dynamic connectedness based on time-varying parameter vector autoregressions. *Journal of Risk and Financial Management*, 13(4):84.

Antonakakis, N., Gupta, R., and Tiwari, A. K. (2017). Has the correlation of inflation and stock prices changed in the United States over the last two centuries? *Research in International Business and Finance*, 42:1–8.

Balcilar, M., Gabauer, D., and Umar, Z. (2021). Crude oil futures contracts and commodity markets: New evidence from a TVP-VAR extended joint connectedness approach. *Resources Policy*, 73:102219.

Boubaker, S., Goodell, J. W., Pandey, D. K., and Kumari, V. (2022). Heterogeneous impacts of wars on global equity markets: Evidence from the invasion of Ukraine. *Finance Research Letters*, 48:102934.

Caldara, D., Conlisk, S., Iacoviello, M., and Penn, M. (2023). Do geopolitical risks raise or lower inflation? Technical report, Federal Reserve Board of Governors.

Caldara, D. and Iacoviello, M. (2022). Measuring geopolitical risk. *American Economic Review*, 112(4):1194–1225.

Chatziantoniou, I. and Gabauer, D. (2021). EMU risk-synchronisation and financial fragility through the prism of dynamic connectedness. *The Quarterly Review of Economics and Finance*, 79:1–14.

D'Agostino, R. B. (1970). Transformation To Normality Of The Null Distribution Of G1. *Biometrika*, 57(3):679–681.

Diebold, F. X. and Yılmaz, K. (2009). Measuring Financial Asset Return And Volatility Spillovers, With Application To Global Equity Markets. *Economic Journal*, 119(534):158–171.

Diebold, F. X. and Yılmaz, K. (2012). Better To Give Than To Receive: Predictive Directional Measurement Of Volatility Spillovers. *International Journal Of Forecasting*, 28(1):57–66.

Diebold, F. X. and Yılmaz, K. (2014). On The Network Topology Of Variance Decompositions: Measuring The Connectedness Of Financial Firms. *Journal Of Econometrics*, 182(1):119–134.

Elliott, G., Rothenberg, T. J., and Stock, J. H. (1996). Efficient Tests For An Autoregressive Unit Root. *Econometrica*, 64(4):813–836.

Fisher, T. J. and Gallagher, C. M. (2012). New weighted portmanteau statistics for time series doodness of fit testing. *Journal of the American Statistical Association*, 107(498):777–787.

Ftiti, Z., Guesmi, K., Nguyen, D. K., and Teulon, F. (2015). Modelling inflation shifts and persistence in Tunisia: perspectives from an evolutionary spectral approach. *Applied Economics*, 47:6200–6210.

Gabauer, D. (2021). Dynamic measures of asymmetric & pairwise connectedness within an optimal currency area: Evidence from the ERM I system. *Journal of Multinational Financial Management*, 60:100680.

Jarque, C. M. and Bera, A. K. (1980). Efficient Tests For Normality, Homoscedasticity And Serial Independence Of Regression Residuals. *Economics Letters*, 6(3):255–259.

Jordan, T. J. (2016). The impact of international spillovers on swiss inflation and the exchange rate. *Journal of International Money and Finance*, 68:262–265.

Koop, G. and Korobilis, D. (2013). Large time-varying parameter vars. *Journal of Econo-*

metrics, 177(2):185–198.

Koop, G. and Korobilis, D. (2014). A New Index Of Financial Conditions. *European Economic Review*, 71:101–116.

Koop, G., Pesaran, M. H., and Potter, S. M. (1996). Impulse Response Analysis In Nonlinear Multivariate Models. *Journal Of Econometrics*, 74(1):119–147.

Lastrapes, W. D. and Wiesen, T. F. (2021). The joint spillover index. *Economic Modelling*, 94:681–691.

Pesaran, H. H. and Shin, Y. (1998). Generalized Impulse Response Analysis In Linear Multivariate Models. *Economics Letters*, 58(1):17–29.

Pham, B. T. and Sala, H. (2022). Cross-country connectedness in inflation and unemployment: measurement and macroeconomic consequences. *Empirical Economics*, 62:1123–1146.

Saâdaoui, F., Jabeur, S. B., and Goodell, J. W. (2022). Causality of geopolitical risk on food prices: Considering the russo-ukrainian conflict. *Finance Research Letters*, 49:103103.

Shahzad, U., Mohammed, K. S., Tiwari, S., Nakonieczny, J., and Nesterowicz, R. (2023). Connectedness between geopolitical risk, financial instability indices and precious metals markets: Novel findings from russia ukraine conflict perspective. *Resources Policy*, 80:103190.

Sim, N. and Zhou, H. (2015). Oil prices, US stock return, and the dependence between their quantiles. *Journal of Banking & Finance*, 55:1–8.

Tiwari, A. K., Shahbaz, M., Hasim, H. M., and Elheddad, M. M. (2019). Analysing the spillover of inflation in selected euro-area countries. *Journal of Quantitative Economics*, 17:551–577.

Table 1: Summary statistics

YoY inflation	USA	CAN	GBR	DEU	BEL	NLD	FRA	ITA	ESP	PRT	GRC
Mean	3.813	3.791	5.176	2.690	3.562	3.425	4.065	5.758	6.429	8.080	8.016
Variance	8.177	9.297	24.084	3.655	8.362	7.017	13.777	31.083	32.067	69.161	66.705
Skewness	1.478***	1.231***	2.010***	0.982***	1.602***	1.127***	1.277***	1.416***	1.193***	1.395***	0.867***
Ex.Kurtosis	2.216***	0.703***	4.148***	0.678***	3.045***	0.816***	0.686***	1.162***	1.078***	1.769***	-0.268
JB	421.492***	202.426***	1030.215***	133.278***	603.166***	177.265***	215.940***	289.467***	211.554***	336.904***	95.039***
ERS	-1.933*	-1.646*	-2.399**	-1.405	-1.687*	-0.845	-1.598	-1.762*	-1.496	-1.597	-2.276**
$Q(24)$	6387.831***	7194.650***	7088.121***	5684.809***	6099.877***	5862.086***	8098.486***	7749.255***	7509.461***	7049.314***	7379.507***
$Q^2(24)$	6260.181***	7175.107***	5738.953***	4711.938***	5451.409***	4896.902***	7432.168***	6542.569***	6854.058***	4452.155***	5630.578***

| Kendall's τ	USA	CAN	GBR	DEU	BEL	NLD	FRA	ITA	ESP	PRT	GRC
USA	1.000***	0.647***	0.564***	0.458***	0.541***	0.391***	0.575***	0.493***	0.513***	0.550***	0.461***
CAN	0.647***	1.000***	0.550***	0.400***	0.540***	0.381***	0.623***	0.534***	0.559***	0.585***	0.457***
GBR	0.564***	0.550***	1.000***	0.544***	0.565***	0.456***	0.666***	0.604***	0.597***	0.600***	0.456***
DEU	0.458***	0.400***	0.544***	1.000***	0.600***	0.580***	0.555***	0.528***	0.516***	0.439***	0.363***
BEL	0.541***	0.540***	0.565***	0.600***	1.000***	0.573***	0.632***	0.554***	0.585***	0.542***	0.383***
NLD	0.391***	0.381***	0.456***	0.580***	0.573***	1.000***	0.492***	0.436***	0.472***	0.420***	0.230***
FRA	0.575***	0.623***	0.666***	0.555***	0.632***	0.492***	1.000***	0.716***	0.702***	0.652***	0.458***
ITA	0.493***	0.534***	0.604***	0.528***	0.554***	0.436***	0.716***	1.000***	0.760***	0.694***	0.592***
ESP	0.513***	0.559***	0.597***	0.516***	0.585***	0.472***	0.702***	0.760***	1.000***	0.689***	0.535***
PRT	0.550***	0.585***	0.600***	0.439***	0.542***	0.420***	0.652***	0.694***	0.689***	1.000***	0.607***
GRC	0.461***	0.457***	0.456***	0.363***	0.383***	0.230***	0.458***	0.592***	0.535***	0.607***	1.000***

Notes: The table reports key summary statistics. The first panel of the table includes mean, variance, as well as Skewness: D'Agostino (1970) test; Ex.Kurtosis: Anscombe and Glynn (1983) test; JB: Jarque and Bera (1980) normality test; ERS: Elliott et al. (1996) unit-root test; $Q(24)$ and $Q^2(24)$: Fisher and Gallagher (2012) weighted portmanteau test. Kendall's τ is reported in the second panel. ***,**,* denote significance level at 1%, 5% and 10%

Table 2: Averaged connectedness table

|	USA	CAN	GBR	DEU	BEL	NLD	FRA	ITA	ESP	PRT	GRC	FROM others
USA	38.11 (0.00)	9.24 (-17.28)	4.17 (-23.99)	5.83 (-13.47)	4.70 (-14.26)	3.27 (-15.26)	10.23 (-10.29)	4.53 (-16.82)	10.62 (-1.90)	6.86 (0.07)	2.44 (-7.29)	61.89
CAN	26.52 (17.28)	21.86 (0.00)	4.11 (-0.17)	5.82 (2.23)	4.36 (-1.03)	3.47 (0.77)	10.54 (5.67)	3.55 (-0.85)	10.07 (5.92)	6.98 (3.63)	2.73 (-0.24)	78.14
GBR	28.16 (23.99)	4.28 (0.17)	20.18 (0.00)	6.14 (-1.07)	8.21 (4.61)	2.79 (-3.49)	11.62 (6.38)	3.54 (-1.18)	6.01 (1.54)	6.03 (2.42)	3.03 (-1.35)	79.82
DEU	19.30 (13.47)	3.58 (-2.23)	7.21 (1.07)	38.37 (0.00)	8.35 (-5.36)	2.62 (-9.41)	7.65 (-1.38)	2.63 (-9.85)	5.04 (-5.52)	2.34 (-3.45)	2.91 (-5.15)	61.63
BEL	18.96 (14.26)	5.39 (1.03)	3.60 (-4.61)	13.71 (5.36)	19.17 (0.00)	4.91 (-5.67)	17.17 (12.99)	3.42 (-0.36)	5.96 (1.48)	3.58 (0.85)	4.13 (0.10)	80.83
NLD	18.54 (15.26)	2.70 (-0.77)	6.28 (3.49)	12.03 (9.41)	10.58 (5.67)	24.24 (0.00)	10.77 (7.72)	2.64 (0.00)	4.09 (0.08)	2.98 (-0.14)	5.16 (2.77)	75.76
FRA	20.52 (10.29)	4.88 (-5.67)	5.24 (-6.38)	9.03 (1.38)	4.19 (-12.99)	3.05 (-7.72)	24.27 (0.00)	6.55 (-10.58)	6.87 (-6.34)	10.06 (0.46)	5.36 (1.49)	75.73
ITA	21.36 (16.82)	4.40 (0.85)	4.71 (1.18)	12.48 (9.85)	3.77 (0.36)	2.63 (0.00)	17.13 (10.58)	13.38 (0.00)	6.97 (-3.45)	8.26 (5.44)	4.91 (1.61)	86.62
ESP	12.52 (1.90)	4.15 (-5.92)	4.47 (-1.54)	10.57 (5.52)	4.49 (-1.48)	4.01 (-0.08)	13.21 (6.34)	10.41 (3.45)	23.21 (0.00)	8.87 (3.44)	4.09 (-3.49)	76.79
PRT	6.79 (-0.07)	3.34 (-3.63)	3.61 (-2.42)	5.80 (3.45)	2.72 (-0.85)	3.12 (0.14)	9.60 (-0.46)	2.82 (-5.44)	5.43 (-3.44)	50.71 (0.00)	6.05 (-0.75)	49.29
GRC	9.73 (7.29)	2.97 (0.24)	4.37 (1.35)	8.06 (5.15)	4.03 (-0.10)	2.39 (-2.77)	3.86 (-1.49)	3.30 (-1.61)	7.58 (3.49)	6.80 (0.75)	46.90 (0.00)	53.10
TO others	182.40	44.94	47.79	89.44	55.39	32.26	111.78	43.38	68.64	62.75	40.81	779.60
Inc. own	220.51	66.80	67.98	127.81	74.56	56.50	136.05	56.76	91.85	113.46	87.71	TCI
NET spillovers	120.51	-33.20	-32.02	27.81	-25.44	-43.50	36.05	-43.24	-8.15	13.46	-12.29	70.87
Net pairwise transmission	9	4	4	8	3	2	6	2	5	8	4	

Notes: The table reports results of the TVP-VAR (0.99, 0.99) extended joint connectedness approach with a lag length of order 1 (BIC) and a 60-step-ahead generalized forecast error variance decomposition (Balcilar et al., 2021). The values in parentheses represent the net pairwise directional connectedness measures.

Figure 1: Year-over-year inflation rates
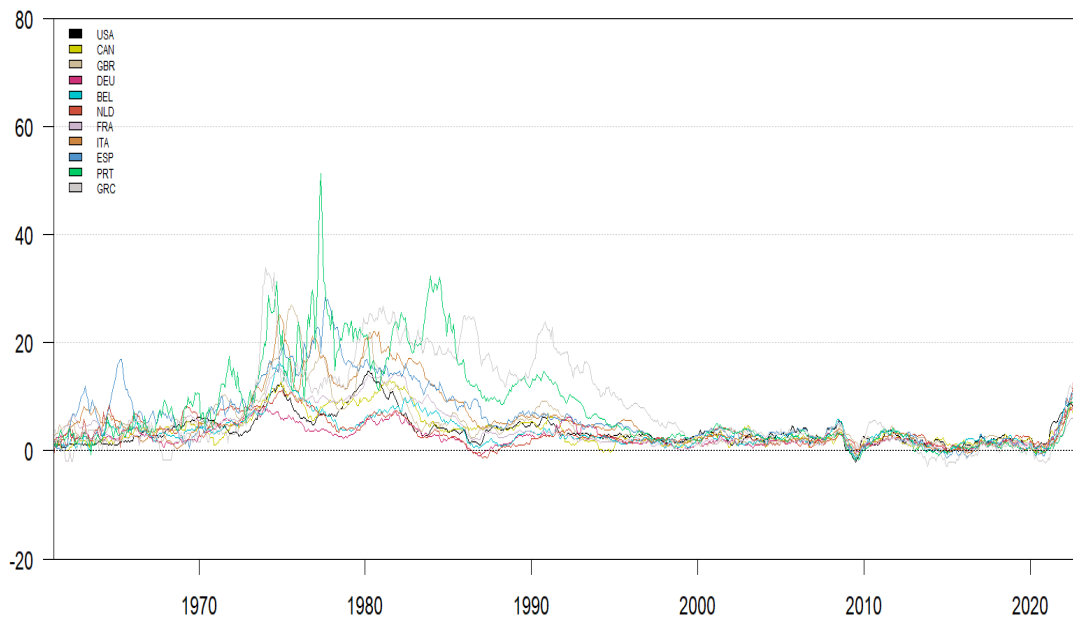
Notes: The figure presents YoY inflation rates calculated from non-seasonally adjusted consumer price indices for the period May 1963 to November 2022. The data has been retrieved from the *Federal Reserve Economic Database.* USA=United States of America, CAN=Canada, GBR=Great Britain, DEU=Germany, BEL=Belgium, NLD=Netherlands, FRA=France, ITA=Italy, ESP=Spain, PRT=Portugal and GRC=Greece.

Figure 2: Net pairwise directional connectedness
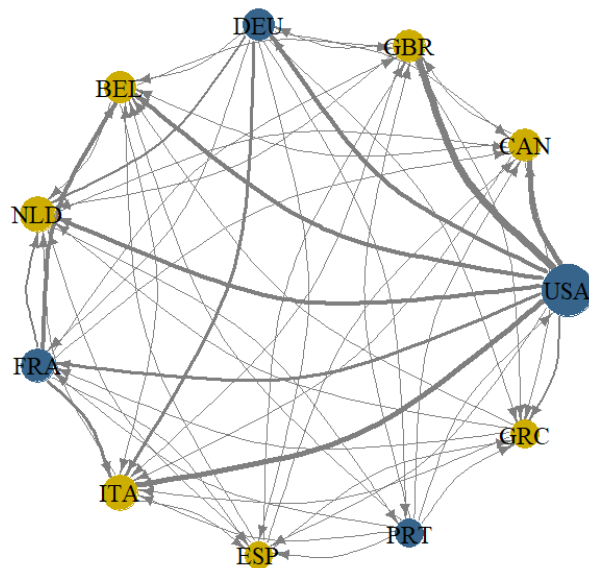
Notes: The figure presents results based on the TVP-VAR extended joint connectedness approach with a lag length of order 1 (BIC) and a 60-step-ahead generalized forecast error variance decomposition (Balcilar et al., 2021). The yellow (blue) circles mark net receivers (transmitters) of shocks.
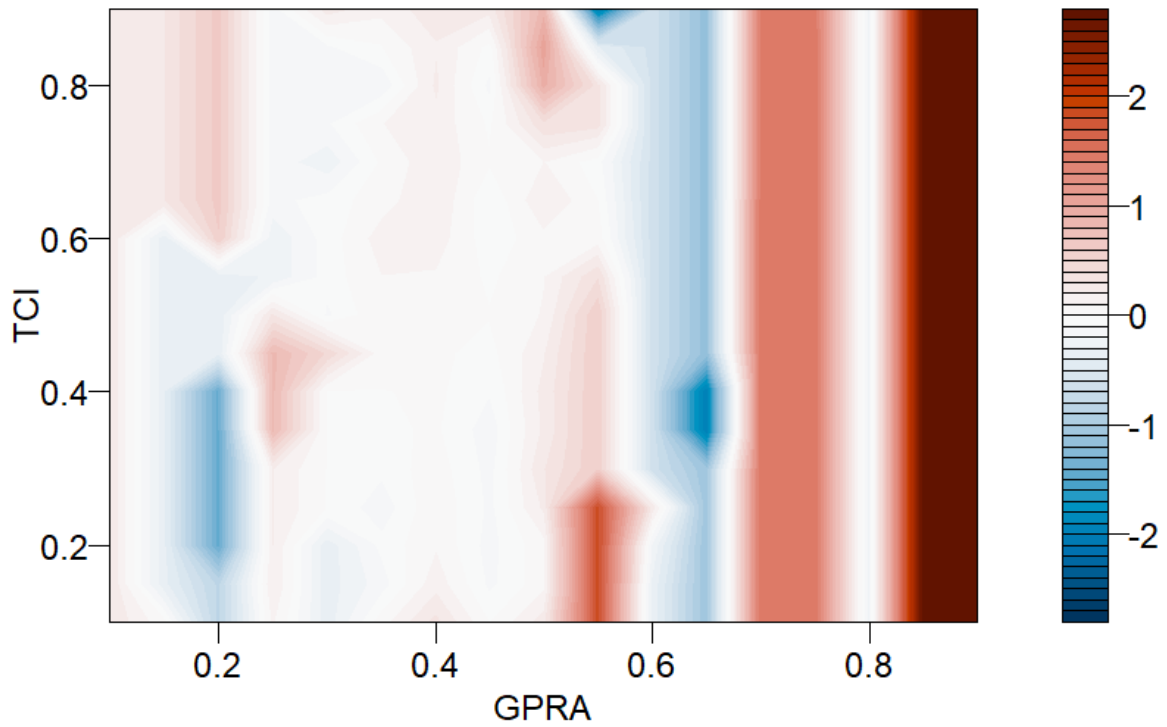
Figure 3: Dynamic total connectedness
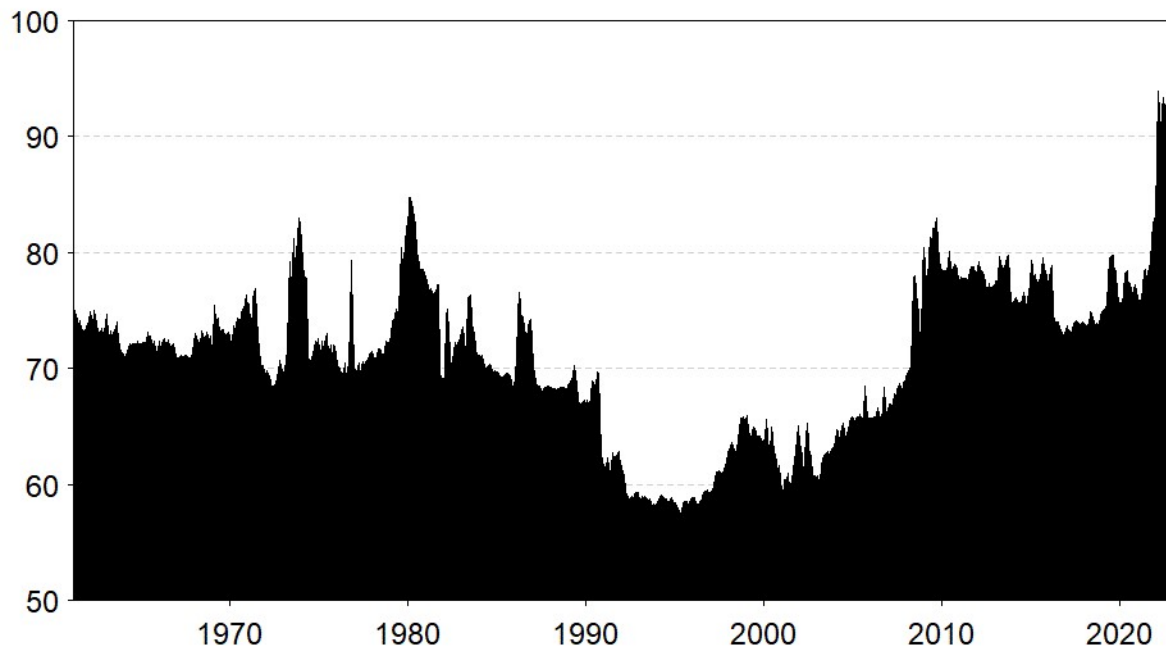
Notes: The figure presents results based on the TVP-VAR extended joint connectedness approach with a lag length of order 1 (BIC) and a 60-step-ahead generalized forecast error variance decomposition (Balcilar et al., 2021).

Figure 4: Quantile-on-quantile between TCI_t and GPR_{t-1}
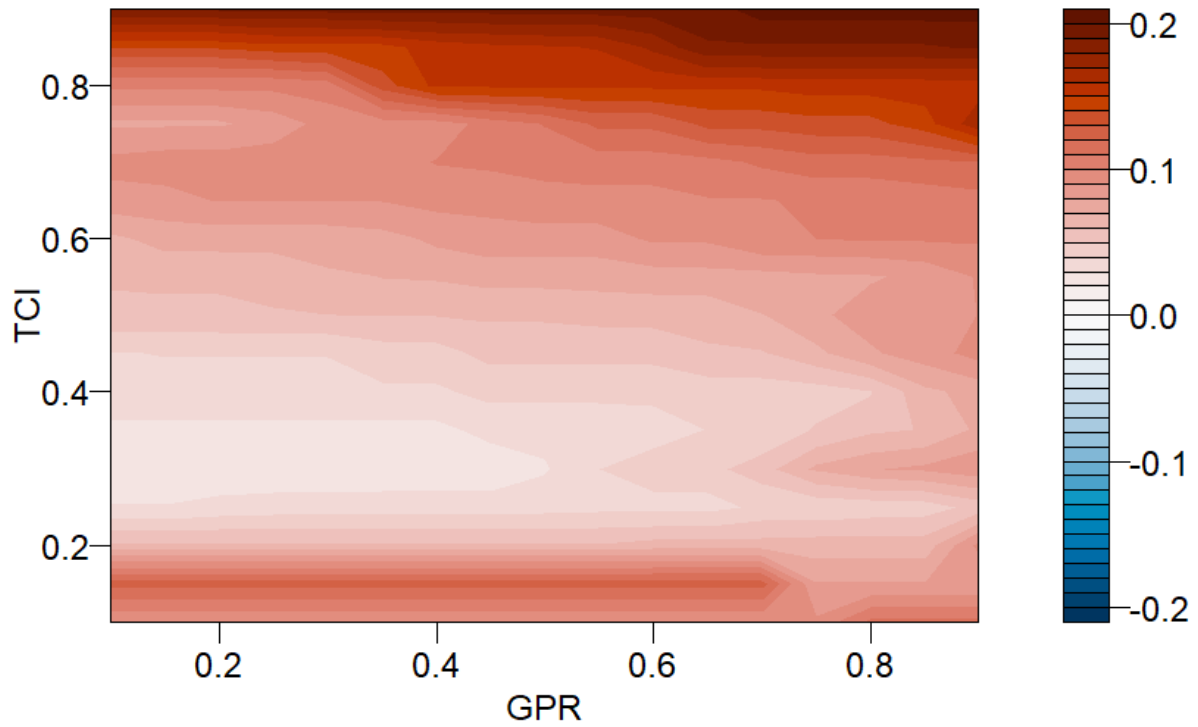
Notes: The figures shows results based on the quantile-on-quantile (QQ) approach of Sim and Zhou (2015). TCI=Total connectedness index, GPR=Geopolitical risk index.

Figure 5: Quantile-on-quantile between TCI_t and $GPRA_{t-1}$

Notes: The figures shows results based on the quantile-on-quantile (QQ) approach of Sim and Zhou (2015). TCI=Total connectedness index, GPRA=Geopolitical risk Acts index.